



Supplement of

Evaluating the impact of enhanced horizontal resolution over the Antarctic domain using a variable-resolution Earth system model

Rajashree Tri Datta et al.

Correspondence to: Rajashree Tri Datta (tri.datta@gmail.com)

The copyright of individual parts of the supplement might differ from the article licence.

Supplementary:

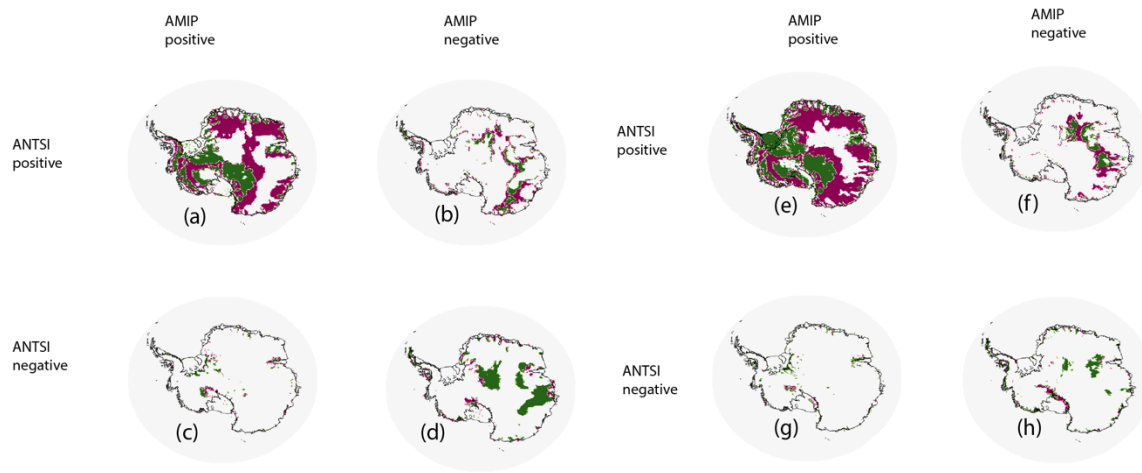
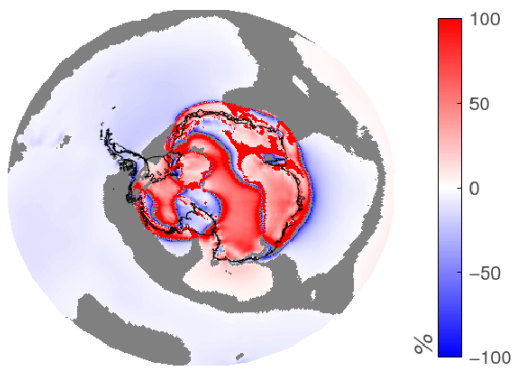


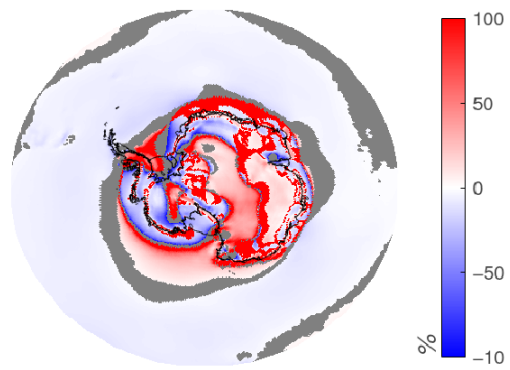
Figure S1: Regions of increased/decreased bias as compared to outside sources. Green indicates where SMB bias is reduced in ANTSI (vs AMIP), purple indicates where SMB bias increased in ANTSI (vs AMIP). With the reconstruction (a)(b)(c)(d), with RACMO2.3 (e)(f)(g)(h)

	Full		Grounded Ice Sheet		Ice Shelves	
	AMIP	ANTSI	AMIP	ANTSI	AMIP	ANTSI
E. Ant	40.20 (±5.69) <i>0.21 GT/yr²</i>	99.43 (±30.42)	10.58 (±1.76) <i>0.07 GT/yr²</i>	34.00 (±10.71)	29.63 (± 4.01) <i>0.14 GT/yr²</i>	59.43 (±20.00)
W. Ant	67.50 (±6.58)	80.41 (±12.43)	16.58 (±2.27) <i>-0.09 GT/yr²</i>	20.67 (±4.09)	50.92 (±4.47)	59.74 (±8.78)
AP	55.71 (±4.56)	53.20 (±9.69)	18.13 (±1.58)	19.83 (±3.09)	37.58 (±3.10)	33.36 (±6.69) <i>0.26 GT/yr²</i>
Total	163.42 (±11.23)	227.04 (±49.66)	45.29 (±3.74)	74.51 (±13.67)	118.13 (±7.70)	152.53 (±27.39)

Table S1: Surface melt values (in GT/yr²) for each region, model source as listed. Interannual trends shown in bold italic using the Mann-Kendall test where p values are < 0.05.



(a) Winter integrated zonal vapor transport (ANTSI - AMIP)



(b) Summer integrated zonal vapor transport (ANTSI - AMIP)

Figure S2: Relative difference (ANTSI-AMIP) for Integrated vapor transport in the zonal direction for (a) winter (b) summer

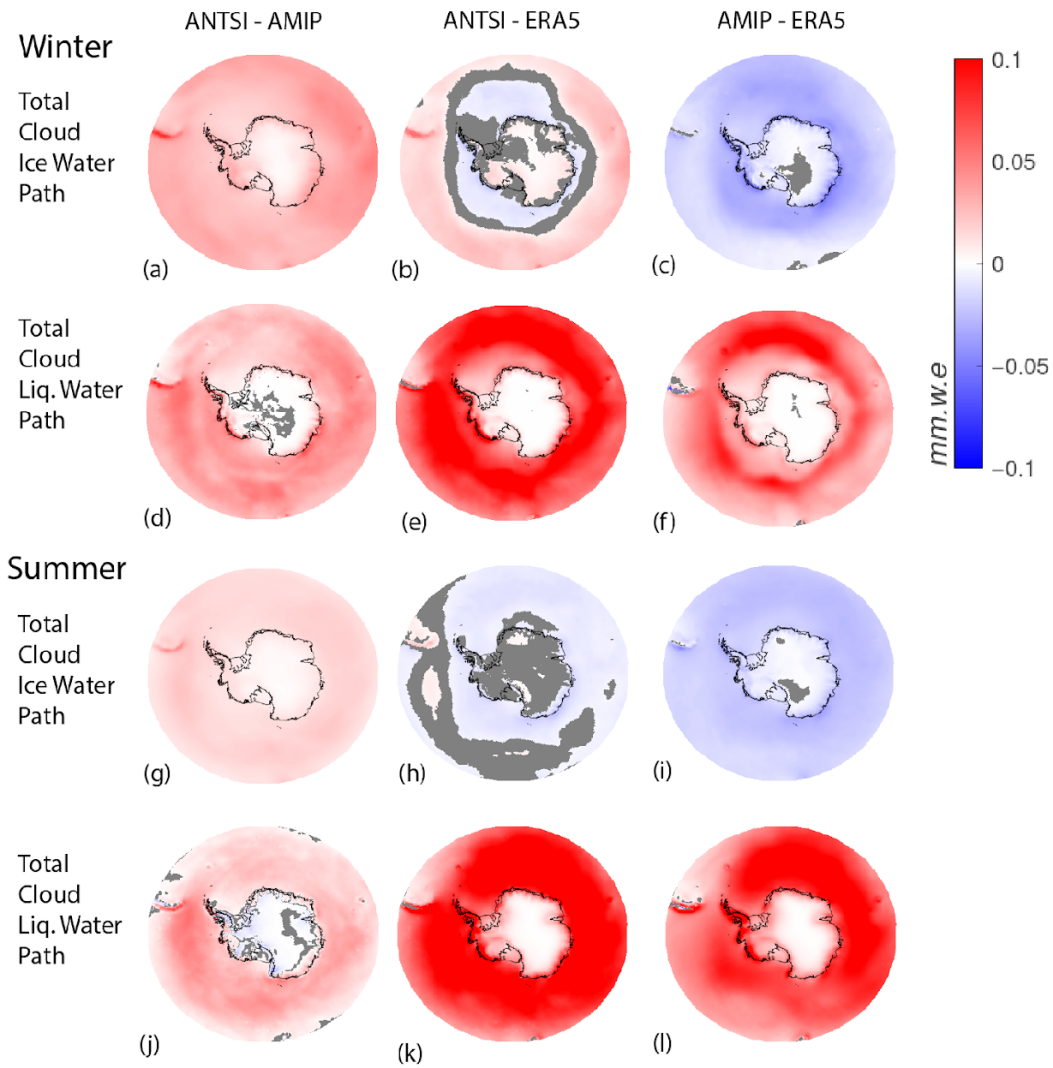


Figure S3: Mean total cloud water path in Winter(JJA) and Summer(DJF) for ANTSI – AMIP (left column), ANTSI-ERA5 (middle column), AMIP-ERA5 (right column). Winter Total Cloud Ice Water Path (a) (b) (c). Winter Total Cloud Liq. Water Path (d) (e) (f). Summer Total Cloud Ice Water Path (g) (h) (i). Summer Total Cloud Liq. Water Path (j) (k) (l).

Reference	Ocean		Ice Sheet	
	Bias +	Bias -	Bias +	Bias -
Winter				
ERA5	0.45 ± 0.74	-1.12 ± 1.11	1.76 ± 1.26	-1.61 ± 1.19
AMIP	0.45 ± 0.56	-0.31 ± 0.38	2.62 ± 1.27	-1.07 ± 0.81
Summer				
ERA5	0.49 ± 0.76	-0.61 ± 0.80	1.59 ± 1.13	-0.68 ± 0.66
AMIP	0.29 ± 0.41	-0.17 ± 0.27	1.11 ± 0.68	-0.64 ± 0.80

Table S2: Mean and standard deviation of near-surface temperature biases (ANTSI - reference dataset) compared to ERA5 and AMIP. Values are separated by season (Winter is JJA, Summer is DJF), by bias direction (positive or negative) and by values over the ocean (below -55°latitude) vs over the ice sheet.

Reference	Ocean		Ice Sheet	
	Bias +	Bias -	Bias +	Bias -
Winter				
ERA5	0.77 ± 0.58	-1.09 ± 0.47	0.13 ± 0.10	-0.57 ± 0.37
AMIP	0.74 ± 0.41	-0.19 ± 0.16	0.98 ± 0.31	no cases
Summer				
ERA5	0.37 ± 0.26	-0.84 ± 0.49	0.19 ± 0.14	-0.30 ± 0.25
AMIP	0.59 ± 0.29	-0.13 ± 0.09	0.96 ± 0.14	no cases

Table S3: 500 hPa temperature biases (ANTSI - reference dataset) in °C, compared to ERA5 and AMIP. Values are separated by season (Winter is JJA, Summer is DJF), by bias direction (positive or negative) and by values over the ocean (below -55°latitude) vs over the ice sheet.

	Ocean		Ice Sheet	
Bias sign	+	-	+	-
Winter				
ERA5	0.72 ± 0.53	-0.81 ± 0.90	1.00 ± 1.13	-0.52 ± 0.30
AMIP	0.32 ± 0.28	-0.66 ± 0.72	0.53 ± 0.55	-0.74 ± 0.77
Summer				
ERA5	0.87 ± 0.58	-0.87 ± 0.87	0.88 ± 0.81	-0.63 ± 0.32
AMIP	0.34 ± 0.31	-0.69 ± 0.74	0.28 ± 0.28	-0.42 ± 0.44

Table S4: 10m windspeed biases (ANTSI - reference dataset) in m/s, compared to ERA5 and AMIP. Values are separated by season (Winter is JJA, Summer is DJF), by bias direction (positive or negative) and by values over the ocean (below -55°latitude) vs over the ice sheet.

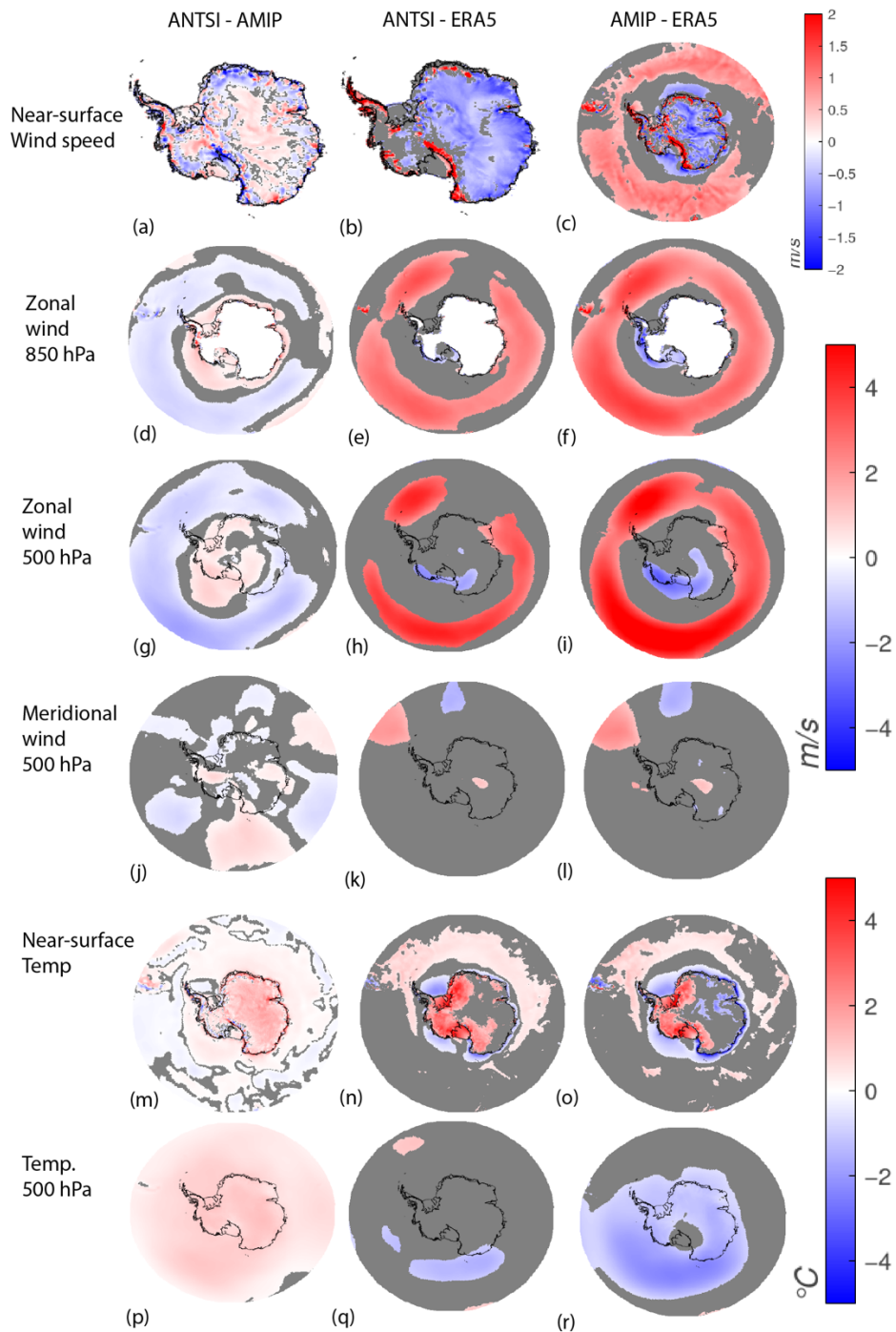


Figure S4: Mean Summer (DJF), 1979-2014 , main climate variables for ANTISI – AMIP (left column), ANTISI-ERA5 (middle column), AMIP-ERA5 (right column). For near- surface wind speed (a)(b)(c), Zonal wind at 850 hPa (d)(e)(f), Zonal wind at 500 hPa, Meridional wind (southward) at 500 hPa (j)(k)(l). Near-surface temperature (m)(n)(o). Temperature at 500 hPa (p)(q)(r). Grey indicates where biases are not significant as compared to AMIP ensemble std dev.

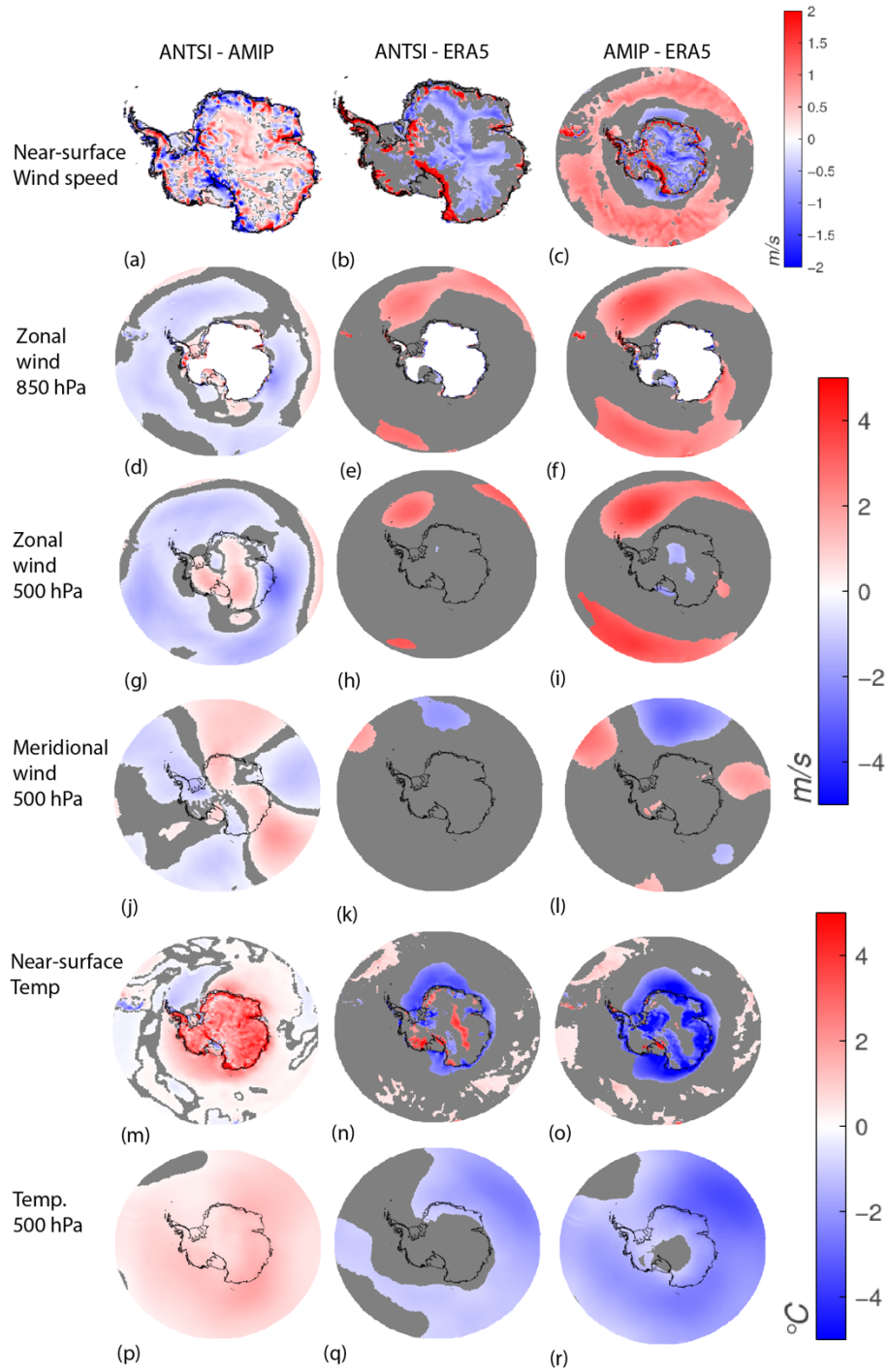


Figure S5: Mean Winter (JJA), 1979-2014 , main climate variables for ANTSI – AMIP (left column), ANTSI-ERA5 (middle column), AMIP-ERA5 (right column). For near- surface wind speed (a)(b)(c), Zonal wind at 850 hPa (d)(e)(f), Zonal wind at 500 hPa, Meridional wind (southward) at 500 hPa (j)(k)(l). Near-surface temperature (m)(n)(o). Temperature at 500 hPa (p)(q)(r). Grey indicates where biases are not significant as compared to AMIP ensemble std dev.

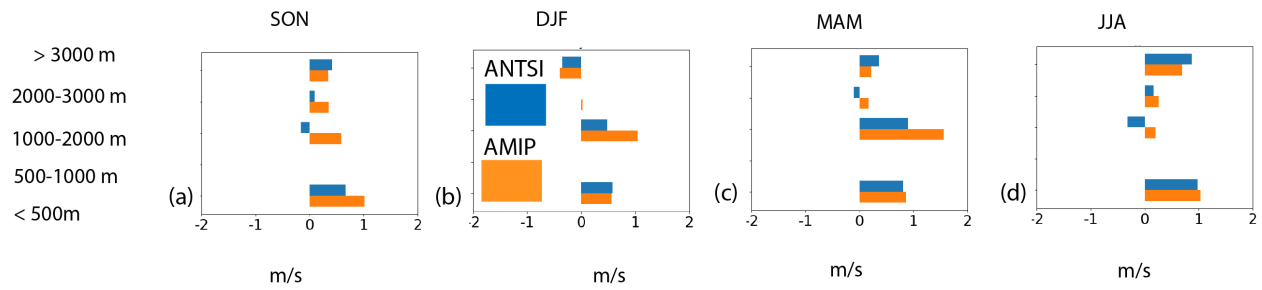


Figure S6: Near-surface wind speed biases as compared to AWS stations, binned into elevation classes (a) SON (b) DJF (c) MAM (d) JJA

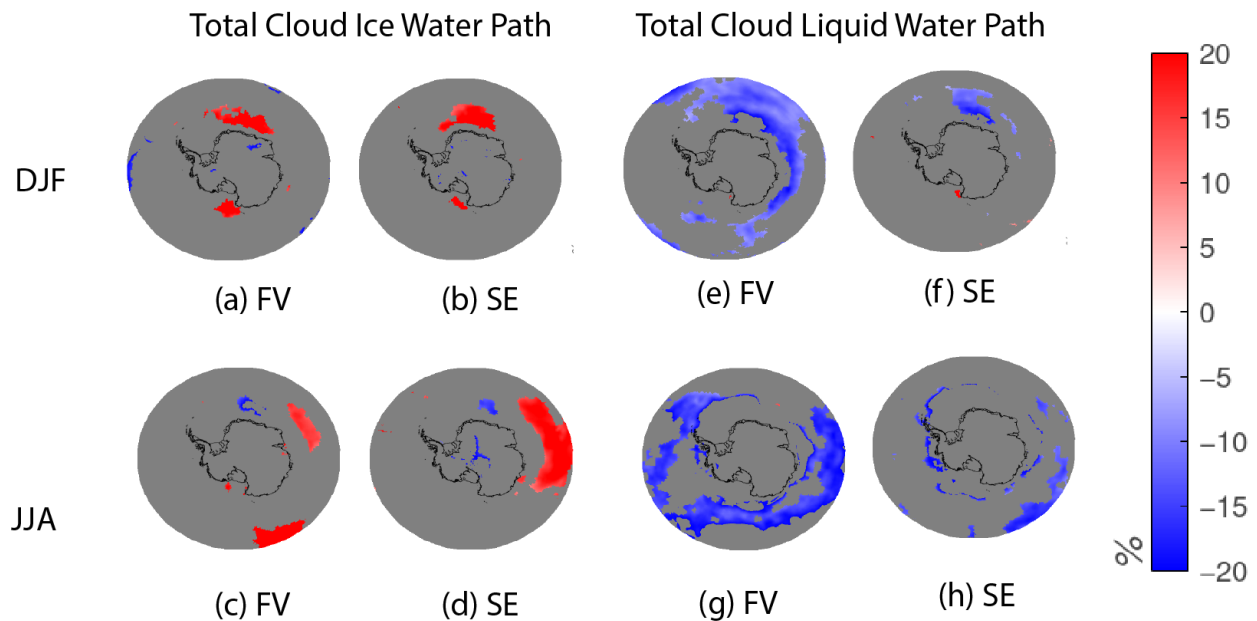


Figure S7: The impact of dynamical core on total cloud water path. Relative change as compared to AMIP-GOGA ensemble means for the period 1978-1998 for two runs at a 1° global spatial resolution, one implementing the finite-volume dynamical core (FV) and the other implementing the spectral element dynamical core (SE). Shown for Total Cloud Ice Water Path (a-d) and Total Cloud Liquid Water Path (e-h), for summer, DJF (a,b,e,f) and winter, JJA (c,d,g,h). Grey indicates where one (temporal) standard deviation of the FV and SE runs do not exceed one (ensemble) standard deviation for AMIP-GOGA

	pattern correlation vs ERA5, SAM DJF	RMS error vs ERA5, SAM DJF	variance explained by DJF SAM	variance explained by monthly SAM	variance explained by PSA1 monthly	variance explained by PSA2 monthly	variance explained by first 3 EOFs monthly
CAM6-ANTSI	0.81	0.51	50.4	27.7	10.8	9.3	47.8
CAM6-SE dycore	0.91	0.34	40.1	23.5	11.5	9.8	44.8
CAM6-FV dycore	0.71	0.51	30.6	22.4	13.2	11.4	47
CAM6-GOGA01	0.77	0.51	46.7	26.2	13.2	11	50.4
CAM6-GOGA02	0.79	0.45	27	26.8	12.6	9.6	49
CAM6-GOGA03	0.75	0.5	38.4	23.2	12.3	10.6	46.1
CAM6-GOGA04	0.7	0.53	32.1	24.5	13.1	10.1	47.7
CAM6-GOGA05	0.9	0.35	39.6	26.9	12.8	10.2	49.9
CAM6-GOGA06	0.78	0.52	48.5	25	10.6	10	45.6
CAM6-GOGA07	0.69	0.52	27.1	25.5	12.1	10.5	48.1
CAM6-GOGA08	0.84	0.45	38.4	23.4	12.1	11.5	47
CAM6-GOGA09	0.77	0.55	46.6	25.6	14	9.5	49.1
CAM6-GOGA10	0.77	0.5	37.9	22.8	12.6	10.6	46
ERA5			40.8	27.8	11.2	9.5	48.5

Table S5. Summary statistics from the Climate Variability Diagnostics Package (see Phillips et al., 2020 and <https://www.cesm.ucar.edu/projects/cvdp>) for the DJF SAM, the monthly SAM, and the monthly PSA-1 and PSA-2 patterns in ERA5 and each of the model configurations considered here. For each dataset, the same number of months were run through the diagnostics. Note that the statistics for CAM6-SE, CAM6-FV, and ANTSI are similar to each other, compare favorably with ERA5, and are within the spread of the AMIP-GOGA ensemble. Rows in bold font correspond to results illustrated in the map plots in Figures S8 and S9.

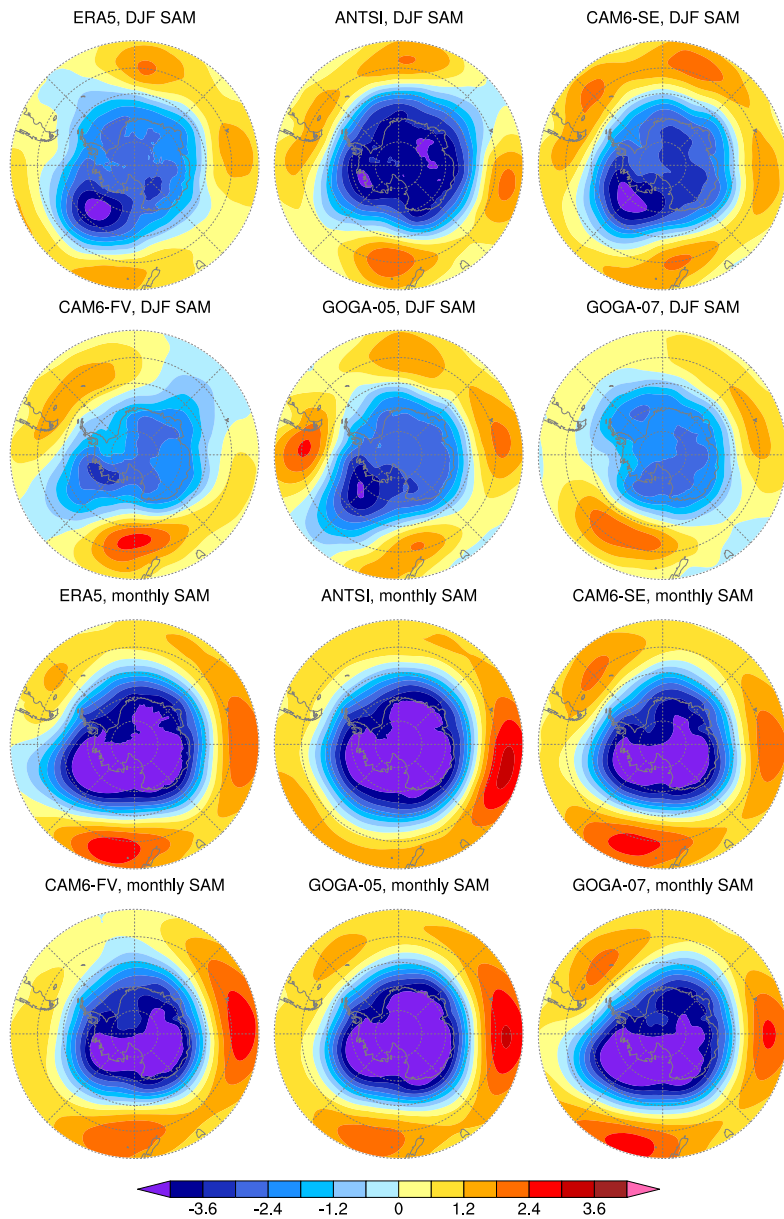


Figure S8: Spatial pattern of the SAM for DJF (top two rows) and monthly (bottom two rows), expressed in sea level pressure anomalies (hPa) corresponding with one positive standard deviation of the SAM index. These results are from the Climate Variability Diagnostics Package.

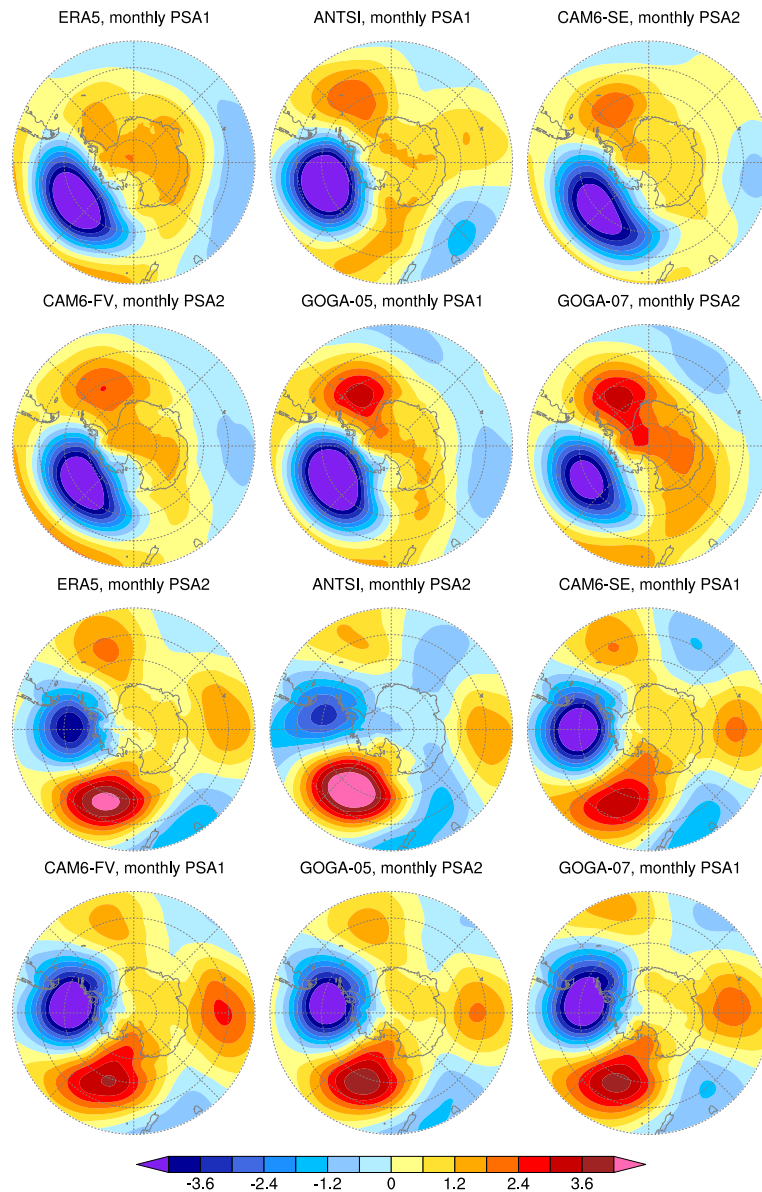


Figure S9: As in Figure S8, but for the PSA-1 and PSA-2 monthly patterns. Note that which pattern is PSA-1 and PSA-2 can vary depending on the dataset considered. The maps have been arranged so that the results are more visually comparable across datasets.

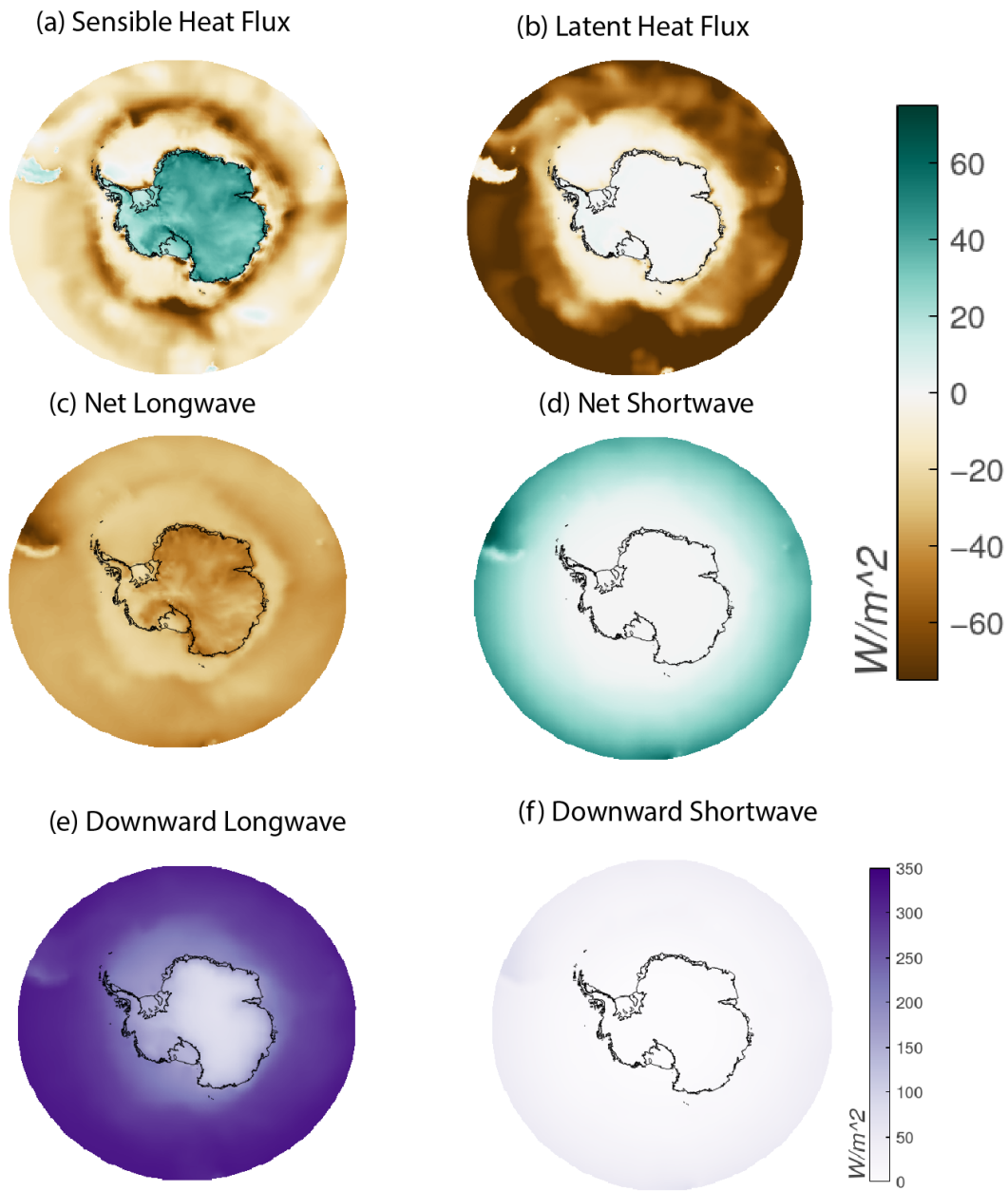


Figure S10: Mean radiation balance for Winter (JJA) from ANTSI, 1979-2014. All values directed towards the surface. For (a) Sensible Heat Flux (b) Latent Heat Flux (c) Net Longwave Radiation (d) Net Shortwave Radiation (e) Downward Longwave Radiation (f) Downward Shortwave Radiation

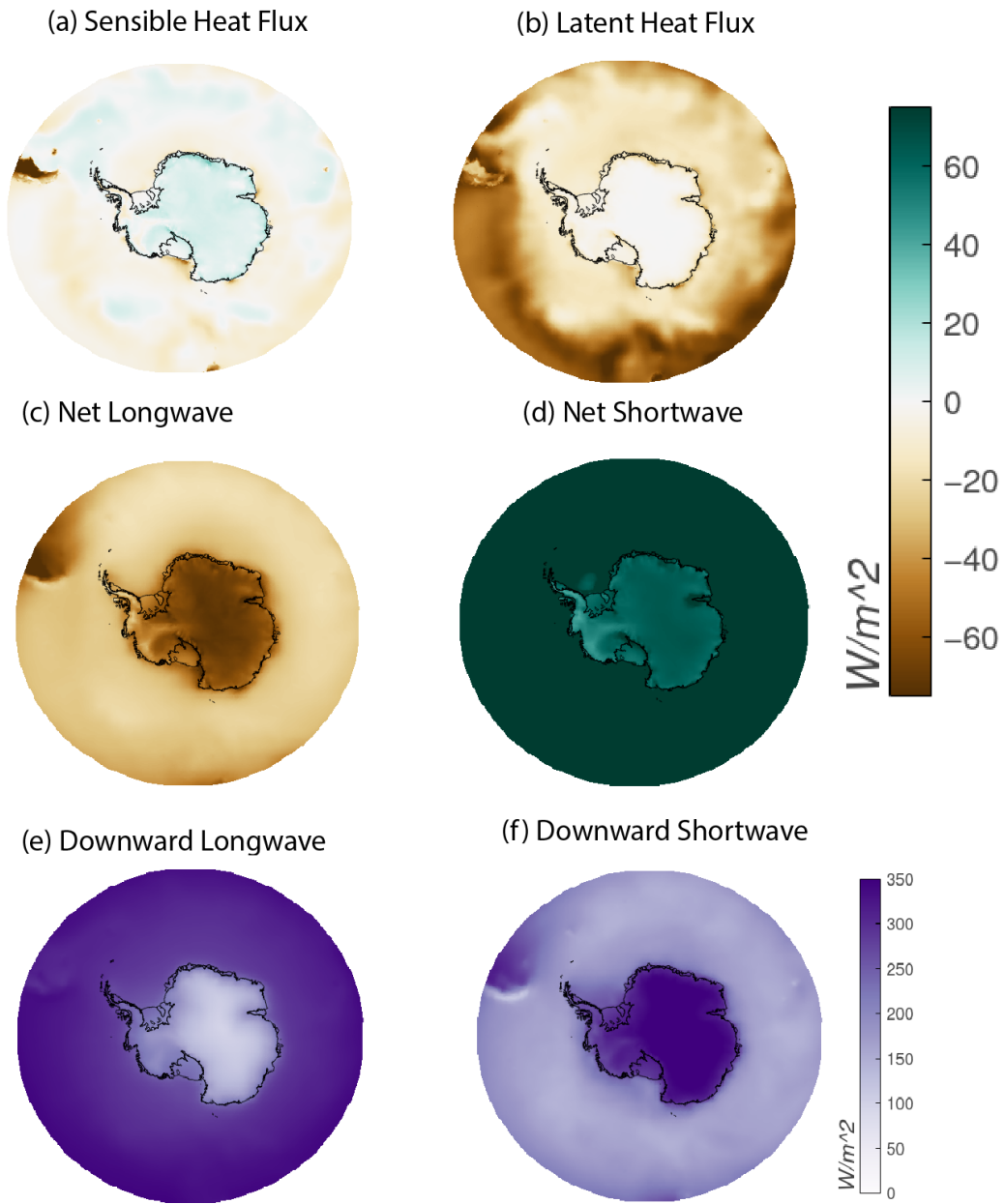


Figure S11: Mean radiation balance for Summer (DJF) from ANTSI, 1979-2014. All values directed at the surface. For (a) Sensible Heat Flux (b) Latent Heat Flux (c) Net Longwave Radiation (d) Net Shortwave Radiation (e) Downward Longwave Radiation (f) Downward Shortwave Radiation

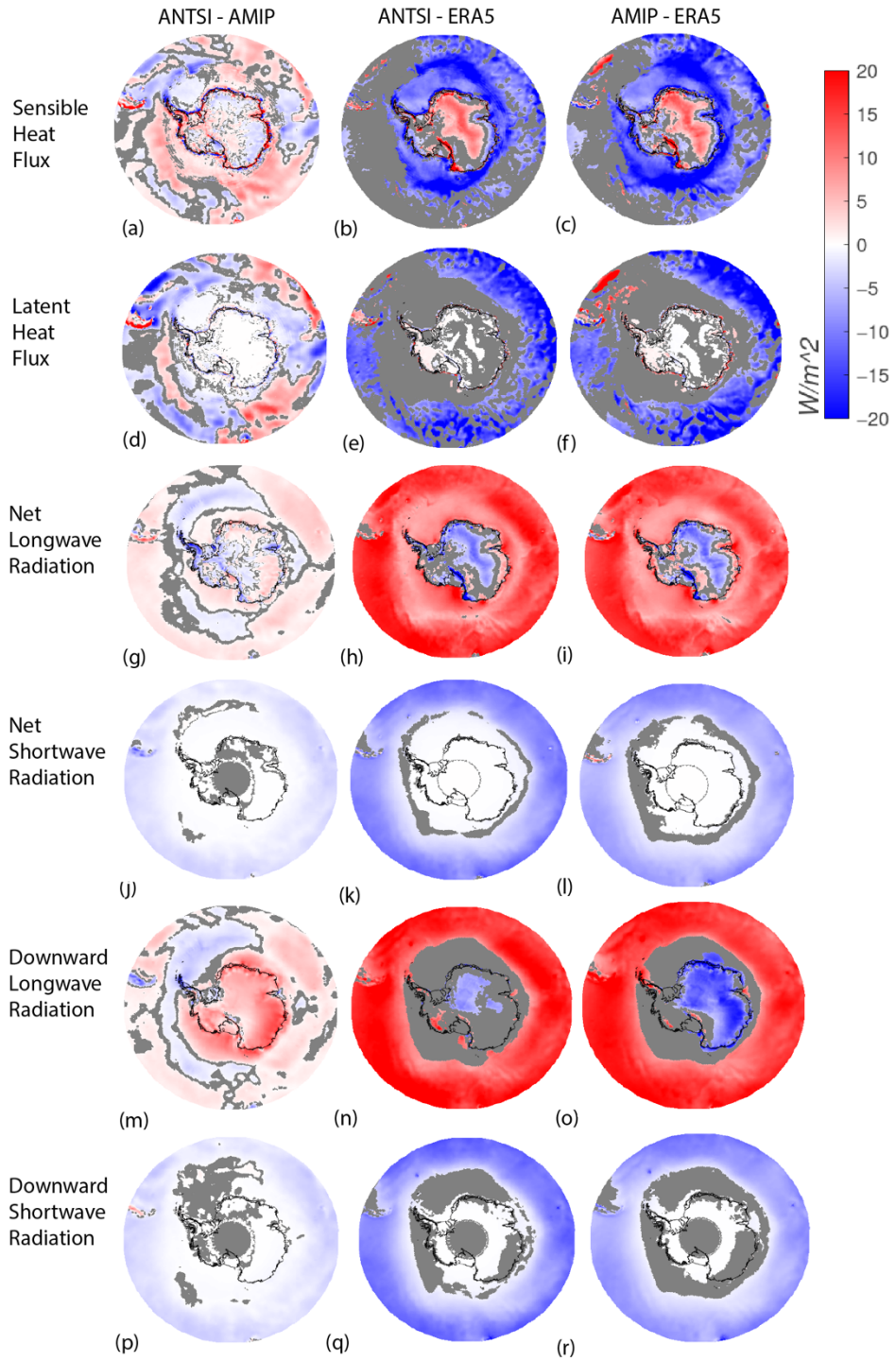


Figure S12: Winter (JJA) radiation balance comparisons, for ANTSI-AMIP (left column), ANTSI – ERA5 (middle column), AMIP-ERA5 (right column). For sensible heat flux (a)(b)(c), latent heat flux (d)(e)(f), net longwave radiation (g)(h)(i), net shortwave radiation (j)(k)(l), downward longwave radiation (m)(n)(o), downward shortwave radiation (p)(q)(r). Grey indicates where biases are not significant as compared to AMIP ensemble std dev.

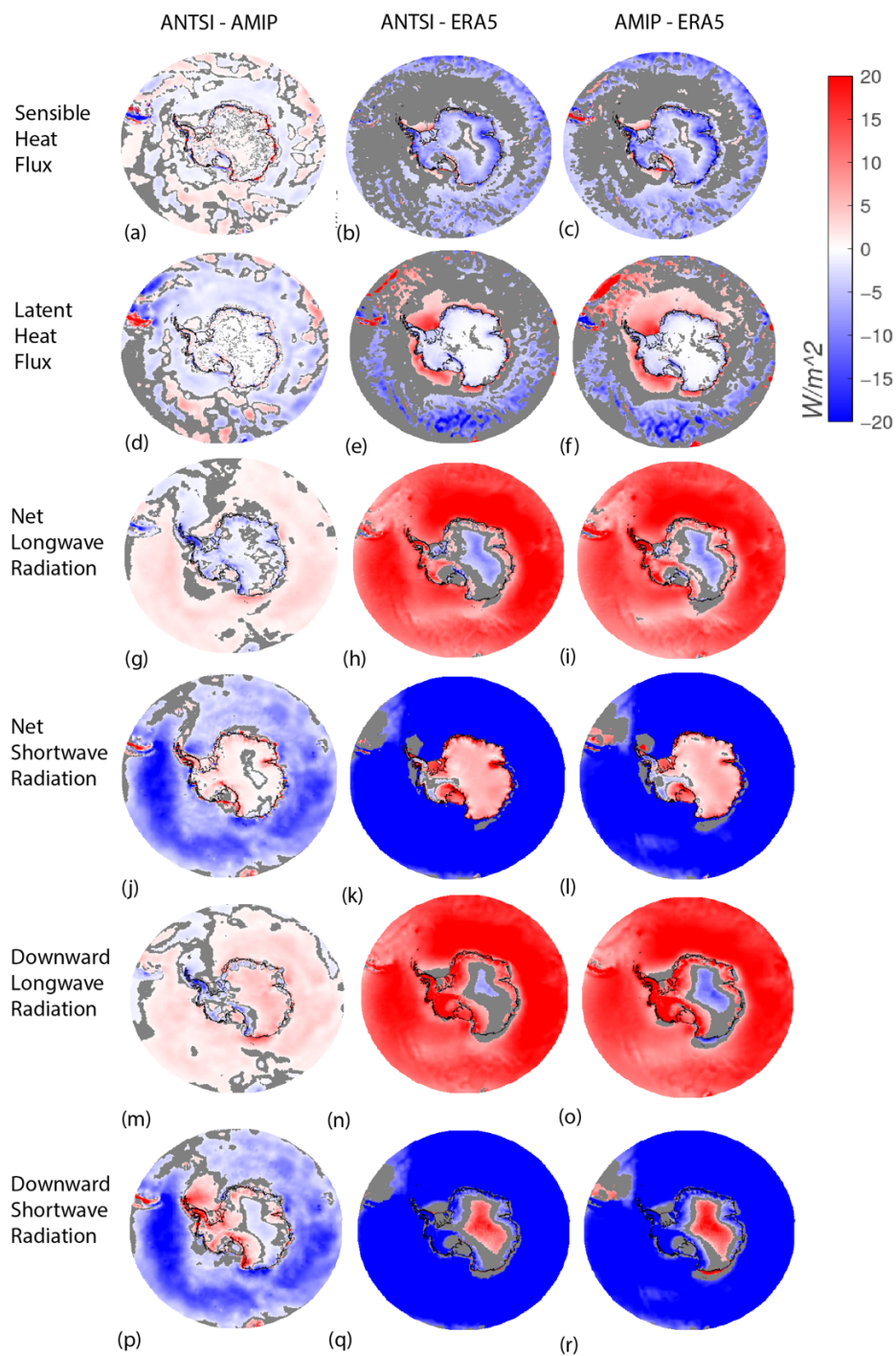


Figure S13: Summer (DJF) radiation balance comparisons, for ANTISI-AMIP (left column), ANTISI – ERA5 (middle column), AMIP-ERA5 (right column). For sensible heat flux (a)(b)(c), latent heat flux (d)(e)(f), net longwave radiation (g)(h)(i), net shortwave radiation (j)(k)(l), downward longwave radiation (m)(n)(o), downward shortwave radiation (p)(q)(r). Grey indicates where biases are not significant as compared to AMIP ensemble std dev.